International Journal of
INTELLIGENT SYSTEMS AND APPLICATIONS IN ENGINEERING
ISSN:2147-6799 www.ijisae.org Original Research Paper

Impact of Zinc Oxide on the Structural and Dielectric Properties of NiO/ZnO Composites

Bushra A. Hasan[1] and Ahmad A. andSara S. Mahmood[2]

Submitted: 30/01/2023 **Accepted:** 03/04/2023

Abstract: The a.c conductivity and dielectric properties of the prepared composites NiO:ZnO composites samples with various mixing ratios (100:0,80:20,60:40,40:60,20:80 and 0:100) wt. % were carried out . The structure phase, the crystallite size and purity of the fabricated NiO:ZnO composites were confirmed using x-ray diffraction pattern. The results declared that the diffraction spectrum of composites samples were compatible with cubic and hexagonal structures phases for 100%NiOand ZnO respectively while the spectrum were compatible with both phases for the residual composites samples. The crystallite size of the most pronounced plane (101) for crystal growth was changed from 23 nm to 49 .4 nm by increasing of mixing ratio of ZnO from 0 to 100wt%. The dielectric properties were studied as function of frequency in the range (50-50x10^6Hz). The a.c conductivity $\sigma_{a.c}(\omega)$ showed power low dependence for the full frequency range except the composite's samples 40, 60 %wt. ZnO where there was d.c region in low frequency region range. The exponent (s) values get to change in non-regular sequence as a result of the increasing of ZnO ratio. The real and imaginary dielectric constant ε_1 and ε_2 were found to increase in non-regular sequence by continuous addition of ZnO to the host oxide. The potential barrier (W_m)for hopping was found to reduce while the density of states at Fermi level N(E_f)was found to increase non- systematically by increasing of ZnO ratio. The values of polarizability (α) were calculated and explained.

Key words: *XRD of NiO/ZnO composites, a.c conductivity, density of states at Fermi level.*

Introduction

Nickel oxide (NiO) is which an intrinsic p-type semiconductor possesses interesting properties like wide energy gap of 4.3 eV, chemical stability and well thermal conductivity. NiO was appointed as photocathode material in dye synthesized solar cell (DSSCs) p-type, tandem dye synthesized solar cell DSSCs and also in organic bulk heterojunction and perovskite heterojunction solar cells as a hole collector in [1]. Zinc oxide (ZnO) is p type semiconductor, due to possess unique traits like a band gap of (3.37 eV), and high binding energy of excitation (60meV) has numerous applications such as LED light emitting diodes, gas sensors, drug transfer and in field effect transistors(FET) [2, 3]. In the present research, we tend to investigate the effect of mixing ratio of NiO/ZnO composites on the structural, a.c conductivity and the real imaginary dielectric constant.

Materials and methodology

Various composites samples from NiO and ZnO were provided from Sigma Aldrich with various mixing ratios (80:20,60:40,40:60,20:80 and 100 wt. %) were synthesis using solid solution method. The composites samples were put in an oven and sintered at 1273 K for five hours. The composites samples were subjected to grinding to obtain and then pressed in pellets shape in one cm in diameter and 0.5 cm in thickness. The loss, capacitance, and resistance were obtained from the LCR meter type Hewlett Packard model (HP4274A).as function to frequency in the range (50-50x10^6Hz). The measurements were carried out by insert the samples between two electrodes.

Results and Discussion

The structural analysis of (NiO:ZnO) composites samples with various mixing ratios is shown in figure 1 and Table.1.

[1]*Department of Physics, College of Science, University of Baghdad*
[2]*Ministry of Science and Technology*
bushra_abhasan@yahoo.com

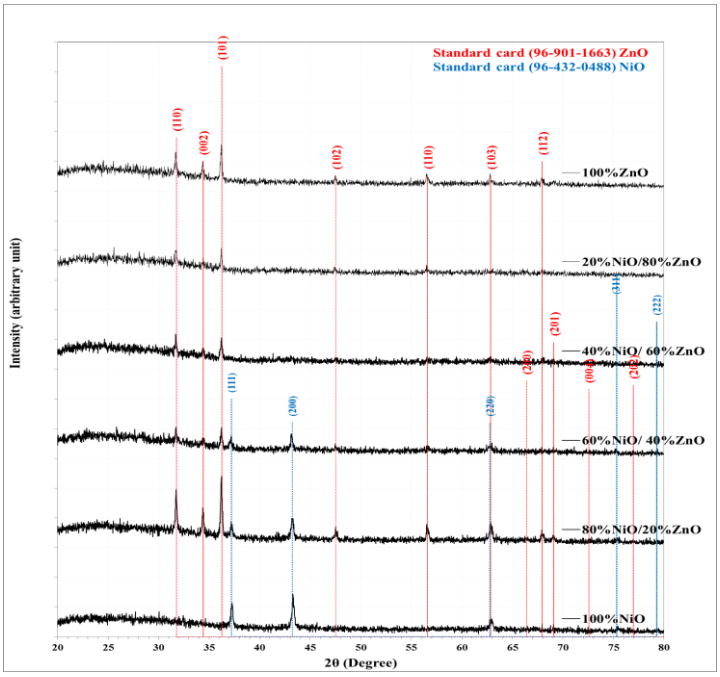

Figure1: The plot of x-ray pattern of (NiO:ZnO) powder with mixing ratios.

The diffraction pattern showed many peaks at two thetas equal 37.24^0 ,43.26^0 ,62.85^0 ,75.40^0 and 79.35^0 which related to planes hkl= (111), (200), (220), (311) and (222). These are compatible with nickel oxide according to the standard card 96-432-0488.It clear that these diffractions peaks still appear at all mixing ratios but disappeared at individual 100%ZnO ratio. On the other side many peaks can be observed at two thetas equal 31.83^0 ,34.50^0 ,36.33^0 ,47.63^0,56,66^0 ,62.69^0 ,66.47^0 ,67.99^0 ,69.14^0 ,72.66^0 and 76.98^0) which belonged to the planed hkl: (100), (002) (101) (102), (110), (103), (200), (112), (201), (004) and (202) respectively which can be seen at all mixing ratios except the individual100% NiO according to the standard card 96-901-1663 [4].

It is obvious that the more pronounced of crystal growth was (200) alters to (101) by increasing of mixing ratio from 0 to 100% ZnO. The crystal size grows up from 23 nm to 49 .4 nm by increasing of ZnO ratio in the mentioned range. Table 1 illustrated the obtained values from x-ray measurement.

Table 1: The x-ray data for NiO/ZnO composites

Nio%	2θ (Deg.)	FWHM (Deg.)	d_{hkl} Exp.(Å)	G.S (nm)	d_{hkl} Std.(Å)	Phase	hkl	card No.
100	37.2492	0.3383	2.4120	24.8	2.4148	Cub. NiO	(111)	96-432-0488
	43.2694	0.3721	2.0893	23.0	2.0913	Cub. NiO	(200)	96-432-0488
	62.8523	0.5073	1.4774	18.4	1.4788	Cub. NiO	(220)	96-432-0488
	75.4002	0.5411	1.2596	18.6	1.2611	Cub. NiO	(311)	96-432-0488
	79.3574	0.4059	1.2065	25.4	1.2074	Cub. NiO	(222)	96-432-0488
80	31.7362	0.2706	2.8172	30.5	2.8137	Hex.ZnO	(100)	96-901-1663
	34.4081	0.2706	2.6043	30.7	2.6035	Hex.ZnO	(002)	96-901-1663
	36.2345	0.2706	2.4771	30.9	2.4754	Hex.ZnO	(101)	96-901-1663
	37.2153	0.4059	2.4141	20.7	2.4148	Cub. NiO	(111)	96-432-0488
	43.2694	0.5411	2.0893	15.8	2.0913	Cub. NiO	(200)	96-432-0488
	47.4972	0.2706	1.9127	32.1	1.9110	Hex.ZnO	(102)	96-901-1663
	56.5614	0.3382	1.6258	26.7	1.6245	Hex.ZnO	(110)	96-901-1663
	62.8523	0.4397	1.4774	21.2	1.4788	Cub. NiO	(220)	96-432-0488
	67.9256	0.3382	1.3788	28.3	1.3782	Hex.ZnO	(112)	96-901-1663
	69.0417	0.2367	1.3593	40.7	1.3582	Hex.ZnO	(201)	96-901-1663
	75.4002	0.6426	1.2596	15.6	1.2611	Cub. NiO	(311)	96-432-0488
	79.3912	0.7440	1.2060	13.9	1.2074	Cub. NiO	(222)	96-432-0488
60	31.8038	0.3044	2.8114	27.1	2.8137	Hex.ZnO	(100)	96-901-1663
	34.4419	0.2367	2.6019	35.1	2.6035	Hex.ZnO	(002)	96-901-1663
	36.2683	0.2367	2.4749	35.3	2.4754	Hex.ZnO	(101)	96-901-1663
	37.2153	0.3044	2.4141	27.5	2.4148	Cub. NiO	(111)	96-432-0488
	43.2356	0.3720	2.0909	23.0	2.0913	Cub. NiO	(200)	96-432-0488
	47.5310	0.2705	1.9114	32.1	1.9110	Hex.ZnO	(102)	96-901-1663
	56.5953	0.3044	1.6249	29.6	1.6245	Hex.ZnO	(110)	96-901-1663
	62.8523	0.4735	1.4774	19.7	1.4788	Cub. NiO	(220)	96-432-0488
	66.4036	0.2368	1.4067	40.1	1.4069	Hex.ZnO	(200)	96-901-1663
	67.9594	0.2368	1.3782	40.5	1.3782	Hex.ZnO	(112)	96-901-1663
	69.0755	0.2367	1.3587	40.7	1.3582	Hex.ZnO	(201)	96-901-1663
	75.3326	0.5073	1.2606	19.8	1.2611	Cub. NiO	(311)	96-432-0488
	79.3236	0.5412	1.2069	19.1	1.2074	Cub. NiO	(222)	96-432-0488

40	31.7700	0.2706	2.8143	30.5	2.8137	Hex.ZnO	(100)	96-901-1663
	34.4419	0.2705	2.6019	30.7	2.6035	Hex.ZnO	(002)	96-901-1663
	36.2683	0.2367	2.4749	35.3	2.4754	Hex.ZnO	(101)	96-901-1663
	37.1815	0.3382	2.4162	24.8	2.4148	Cub. NiO	(111)	96-432-0488
	43.2356	0.3382	2.0909	25.3	2.0913	Cub. NiO	(200)	96-432-0488
	47.5648	0.3044	1.9102	28.5	1.9110	Hex.ZnO	(102)	96-901-1663
	56.5953	0.3044	1.6249	29.6	1.6245	Hex.ZnO	(110)	96-901-1663
	62.8523	0.4397	1.4774	21.2	1.4788	Cub. NiO	(220)	96-432-0488
	66.3698	0.2706	1.4073	35.1	1.4069	Hex.ZnO	(200)	96-901-1663
	67.9256	0.3044	1.3788	31.5	1.3782	Hex.ZnO	(112)	96-901-1663
	69.0755	0.2706	1.3587	35.6	1.3582	Hex.ZnO	(201)	96-901-1663
	75.3326	0.5073	1.2606	19.8	1.2611	Cub. NiO	(311)	96-432-0488
	76.9222	0.2029	1.2385	50.0	1.2377	Hex.ZnO	(202)	96-901-1663
	79.2221	0.5412	1.2082	19.1	1.2074	Cub. NiO	(222)	96-432-0488
20	31.8377	0.2367	2.8085	34.9	2.8137	Hex.ZnO	(100)	96-901-1663
	34.4758	0.2367	2.5994	35.1	2.6035	Hex.ZnO	(002)	96-901-1663
	36.3021	0.2367	2.4727	35.3	2.4754	Hex.ZnO	(101)	96-901-1663
	37.2492	0.3044	2.4120	27.5	2.4148	Cub. NiO	(111)	96-432-0488
	43.2356	0.3044	2.0909	28.1	2.0913	Cub. NiO	(200)	96-432-0488
	47.5986	0.3382	1.9089	25.7	1.9110	Hex.ZnO	(102)	96-901-1663
	56.6291	0.2706	1.6240	33.3	1.6245	Hex.ZnO	(110)	96-901-1663
	62.8861	0.3383	1.4767	27.5	1.4788	Cub. NiO	(220)	96-432-0488
	66.4036	0.2706	1.4067	35.1	1.4069	Hex.ZnO	(200)	96-901-1663
	67.9932	0.3382	1.3776	28.3	1.3782	Hex.ZnO	(112)	96-901-1663
	69.1094	0.3044	1.3581	31.7	1.3582	Hex.ZnO	(201)	96-901-1663
	72.5930	0.2029	1.3013	48.6	1.3017	Hex.ZnO	(004)	96-901-1663
	75.2988	0.4735	1.2611	21.2	1.2611	Cub. NiO	(311)	96-432-0488
	76.9899	0.2029	1.2375	50.0	1.2377	Hex.ZnO	(202)	96-901-1663
	79.3236	0.5411	1.2069	19.1	1.2074	Cub. NiO	(222)	96-432-0488
0	31.8377	0.2368	2.8085	34.9	2.8137	Hex.ZnO	(100)	96-901-1663
	34.5096	0.2367	2.5969	35.1	2.6035	Hex.ZnO	(002)	96-901-1663
	36.3360	0.1691	2.4705	49.4	2.4754	Hex.ZnO	(101)	96-901-1663
	47.6325	0.3044	1.9076	28.5	1.9110	Hex.ZnO	(102)	96-901-1663
	56.6629	0.2706	1.6231	33.4	1.6245	Hex.ZnO	(110)	96-901-1663
	62.9200	0.2367	1.4759	39.3	1.4772	Hex.ZnO	(103)	96-901-1663
	66.4713	0.2367	1.4054	40.1	1.4069	Hex.ZnO	(200)	96-901-1663
	67.9932	0.3382	1.3776	28.3	1.3782	Hex.ZnO	(112)	96-901-1663
	69.1432	0.3044	1.3575	31.7	1.3582	Hex.ZnO	(201)	96-901-1663
	72.6607	0.2706	1.3002	36.4	1.3017	Hex.ZnO	(004)	96-901-1663
	76.9899	0.2029	1.2375	50.0	1.2377	Hex.ZnO	(202)	96-901-1663

a.c conductivity σa.c(ω) study

The overall conductivity was measured using the relation:

$$\sigma_{tot} = \sigma_{a.c}(\omega) + \sigma_{d.c} \quad \ldots (1)$$

The a.c conductivity $\sigma_{a.c}$ obeying the universal feature of the a.c conductivity, thus by subtracting the direct current conductivity σ_{dc} (with the smallest value) from the total conductivity the alternative current conductivity can be obtained using the relation:

$$\sigma_{a.c}(\omega) = \sigma_{tot} - \sigma_{d.c} = A\omega^{s} \quad \ldots (2)$$

where s is the frequency exponent factor, A is a constant, ω is the angular frequency ω = 2πf and f is the frequency range. The variation of a.c conductivity with the angular frequency was studied in the frequency range (50-50MHz). Figure 1 declares the relation between the ac conductivity $\sigma_{ac}(\omega)$ and angular frequency for the composite's samples with different zinc oxide ratio. It is obvious from the figure that that $\sigma_{a.c}(\omega)$ grow up by increasing of angular frequency. Similar behavior was observed by all samples except the composite's samples with 60, and 40 % wt. of zinc oxide i.e. These samples declared frequency independence in the low frequency range or σ_{dc} is dominated at low frequency range. The exponent (s) values can be determined from the slope of figure 2 which were recorded in table 2.

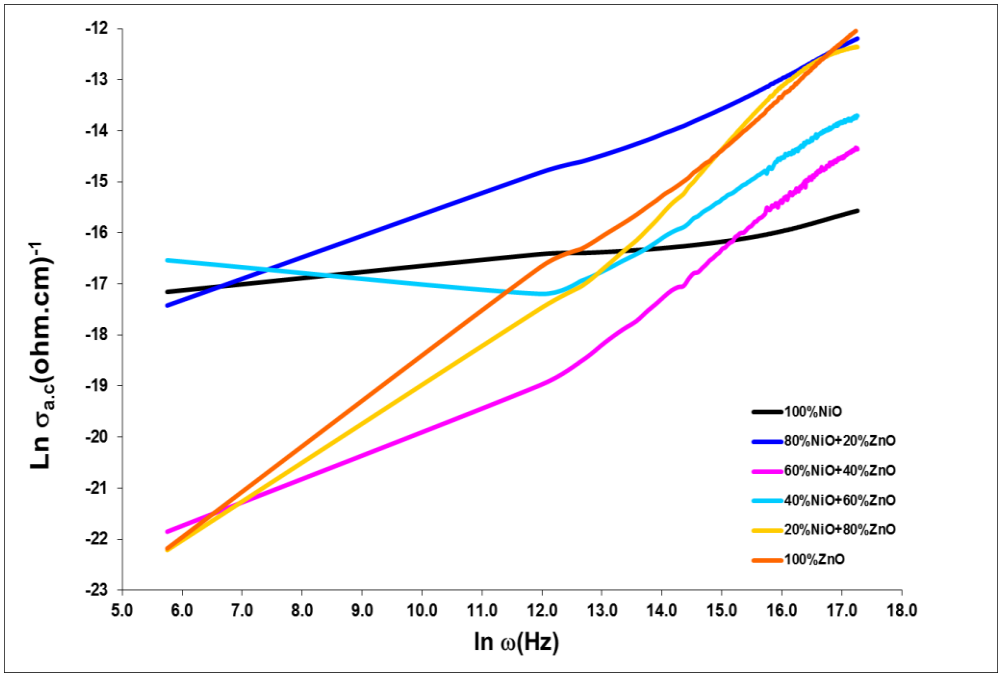

Figure2: The plot of ln $\sigma_{a.c}(\omega)$ versus Ln ((ω) of (NiO/ZnO) with various mixing ratios

It is evident that s value was small for composites with low zinc oxide ratio which confirm hoping mechanism [5], while s was close to unity for composites with high zinc oxide ratio. On the other hand, s values get to change in non-regular manner by increasing of zinc oxide ratio in the composite's samples. The increasing of exponent s suggested that small polaron (SP) is the most convenient model the to explain the behavior of (s) [6]. The correlated barrier hopping (CBH) model [7, 8, 9] suggested a reduction in the exponent s value. This model suggested that the charge carriers will hope over a defect states D+ and D−. It is expected that each pair of defect states will establish a dipole which relaxed over the potential barriers where the carriers jumped over it [10-13]. It is clearly observed that that type of hoping mechanism strongly influenced by N (E_f) which is the density of localized states, N (E_f) can be calculated by the following relation [12]:

$$\sigma_{a.c}(\omega) = \frac{1}{3}\pi e^2 k_B T[N(Ef)]^2 \bar{\alpha}^{-5} \omega[\ln(\nu ph)\omega]^4 \quad \ldots (3)$$

where e, ν_{ph} and $\bar{\alpha}$ are the electronic charge and the predominant phonon frequency and the exponential decay parameter respectively. By suggesting the values of ν_{ph} = 10^{12} Hz and $\bar{\alpha}^{-1}$ = 10 Å [13], N (E_f) was calculated as function of angular frequency for the composites samples and listed in table 1. The increase of zinc oxide content in the composites samples leads to well pronounced increase in the density of localized states which consequently improve the ac conductivity.

Table 2: The values of s, polarizability (α), density of states at Fermi level N(E_f), and the height of the potential barrier W_m for (NiO/ZnO) composites

Nio%	s	At f=50MHz		α	slope	W_m(eV)
		N(E_f)(cm)$^{-3}$	$\sigma_{ac}(\omega)$(ohm.cm)-1			
100	0.184	3.24E+35	1.73x10^{-7}	0.166667	-0.208772	-0.4957566
80	0.521	6.35E+35	5.05x10^{-6}	0.244444	-1.471415	-0.0703405

60	0.806	2.30E+35	$5.78x10^{-7}$	0.055556	-0.022543	-4.591296
40	0.534	3.20E+35	$1.11x10^{-6}$	0.111111	-0.17127	-0.6043032
20	0.952	6.30E+35	$4.27x10^{-6}$	0.366667	-0.282334	-0.3665871
100	0.947	7.49E+35	$5.96x10^{-6}$	0.177778	-2.56E-01	-0.4044859

Dielectric properties ε1(ω) and ε2(ω) studies

The dielectric properties are composed from two main parts (1) the former is represent the ability of materials to store the electrical charge which describes the capacitive (insulating) nature. (2) The later represents the ability to transfer charges which describes the conductive nature.

The relation between the angular frequency and the real dielectric constant $\varepsilon_1(\omega)$ was studied for the composite's samples with various oxide content in the frequency range (50 to 50 $x10^6$ Hz as shown in figure 3. From this figure it is obvious that the real dielectric constant ε_1 decreases by the increasing of frequency. The reduction of the real dielectric constant ε_1 with the increasing of the frequency can be demonstrated depending on the reduction of the four types of the polarization named (electronic, ionic, orientation and space charge) participate to the real dielectric constant. The electronic polarization results from the displacement of valence electrons relative to positive nucleus which take place at frequencies up to 10^{13}–10^{15} Hz. Secondly, ionic polarization results from the displacement of ions forming a hetero polar molecule (negative and positive ions relative) which take place in the frequency range 10^{12}–10^{13} Hz. The third type of polarization, space charge polarization results from the impedance mobile charge carrier by interfaces, this type of polarization take place in the frequency range tween 1 and 10^3 Hz. The summation of these four types of polarization represents the overall polarization [14].

In the present work the ionic polarization has no noticeable participation in the overall polarization. When the frequency is increased, the orientation polarization reduces because the dipoles are not capable follow the applied electric field, so the oscillation will be retarded behind those of the electric field as a result of taking extra time exceeded those of other type of polarization (electronic and ionic polarizations). By increasing the frequency, the constant dipole will be found, which has no ability to peruse the electric field and thus the contribution of the orientation polarization will be completely stopped, consequently the real dielectric constant ε_1 decreases reach constant value and hence the contribution of the interfacial or space charge polarization only.

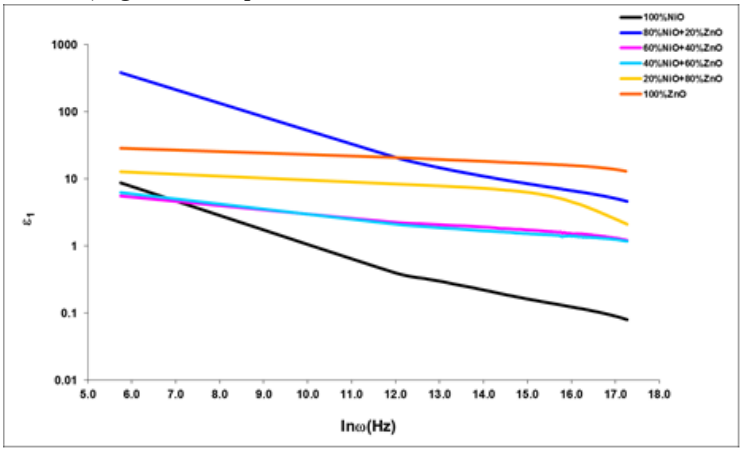

Figure3: The plot of ε_1 versus Ln (ω) of (NiO/ZnO) with various ratios

The relation between the angular frequency and imaginary dielectric loss ε_2 was studied for the composite's samples with different zinc oxide content through the mentioned frequency range as shown in figure 4. The dielectric loss composed from two participations contributions, the former from direct current conduction and the later from the dielectric polarization processes. It is obvious that the dielectric loss is ascribed to a.c conduction neither to dc conduction, i.e., the dielectric loss produced from a.c conduction exceeded that produced from d.c conduction. The deprivations result from a.c conduction may be involving the peregrination of ions over great space in the similar way of motion that happen in direct current. The movement of ions supplied energy which will be dissipated in rate proportional to the a.c conductivity to the angular frequency $\frac{\sigma_{a.c}(\omega)}{\omega}$ [15]. It is evident from

the same figure that the imaginary dielectric constant ε_2 get to decrease by increasing of angular frequency.

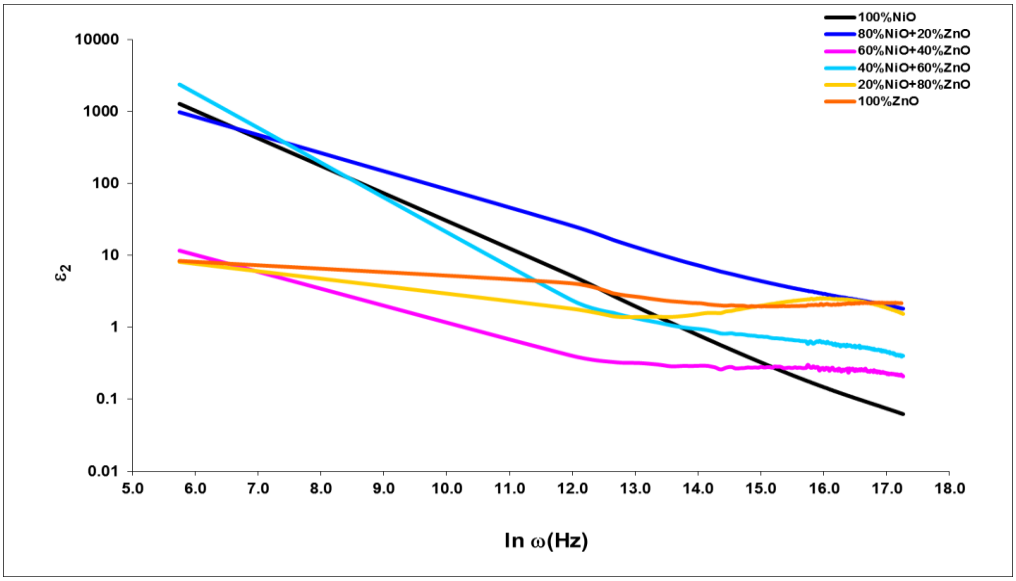

Figure4: The plot of ε_2 versus ln (ω) of (NiO/ZnO) with various ratios

The reduction of imaginary dielectric constant ε_2 with angular frequency is related to the peregrination of the ions which establish the main source of ε_2 in law frequency range. Thus, the participation of ions jumping, polarization loss as well as other conduction loss are responsible about the low value of ε_2 at low and moderate frequencies. However, at high frequencies the ion vibrations may be the only source of the only origin of ε_2. Mott et al. [16] pointed out that when the sample is inserted in an electric field, electron will be jumped between the available localized states. The charge carriers that move between these donors to acceptor sited will form a dipole. The relaxation time of the dipoles depends on the activation energy which originated from the potential barrier W_m where the charge carriers jump over it [10,17]. The potential barrier was suggested by Elliott [7,18] as a result of Columbic interaction between each neighbors' sites forming a dipole. Thus, by using the following relation, the potential barrier can be measured [11]:

$$\varepsilon_2(\omega) = (\varepsilon_o - \varepsilon_\infty)2\pi^2 N(\frac{ne^2}{\varepsilon_o})3k_B T\tau_o{}^m W_m{}^{-4}\omega^m$$

(4) where $m = \dfrac{-4k_B T}{W_m}$ … (5)

where ε_∞ is the infinite frequency dielectric constant, ε_o is the Permittivity of free space =8.854x10^{-14} (F/cm) respectively, and W_m is the energy demand to transfer charge carrier from one site to the infinite. Thus, W_m can be measured from the plot of ln $\varepsilon_2(\omega)$ as function of ln (angular frequency ω). The plot provided a straight line with negative slope.

Figure 8 shows the relation between ln $\varepsilon_2(\omega)$ versus ln (ω) at various zinc oxide ratios values through the frequency range (50 to 50 x10^6 Hz) for the composite's samples (NiO/ZnO) with various ratios. It is obvious that the obtained relations produced straight lines for all composites samples. The power (m) was measured and listed in table 2. It is clear that the slope value (m) decreases non systematically with increasing of zinc oxide ratio in the investigated composites samples. The measured values for Wm are 0.299, 0.0, 4.591, 0.604, 0.22, and 0.429 eV, respectively, for composites samples with zinc oxide ratios in the range 0 to 100 % wt. The calculated values for the potential barrier height Wm are compatible with the theory proposed by Elliott [7, 17] when the charge carriers jump over a potential barrier.

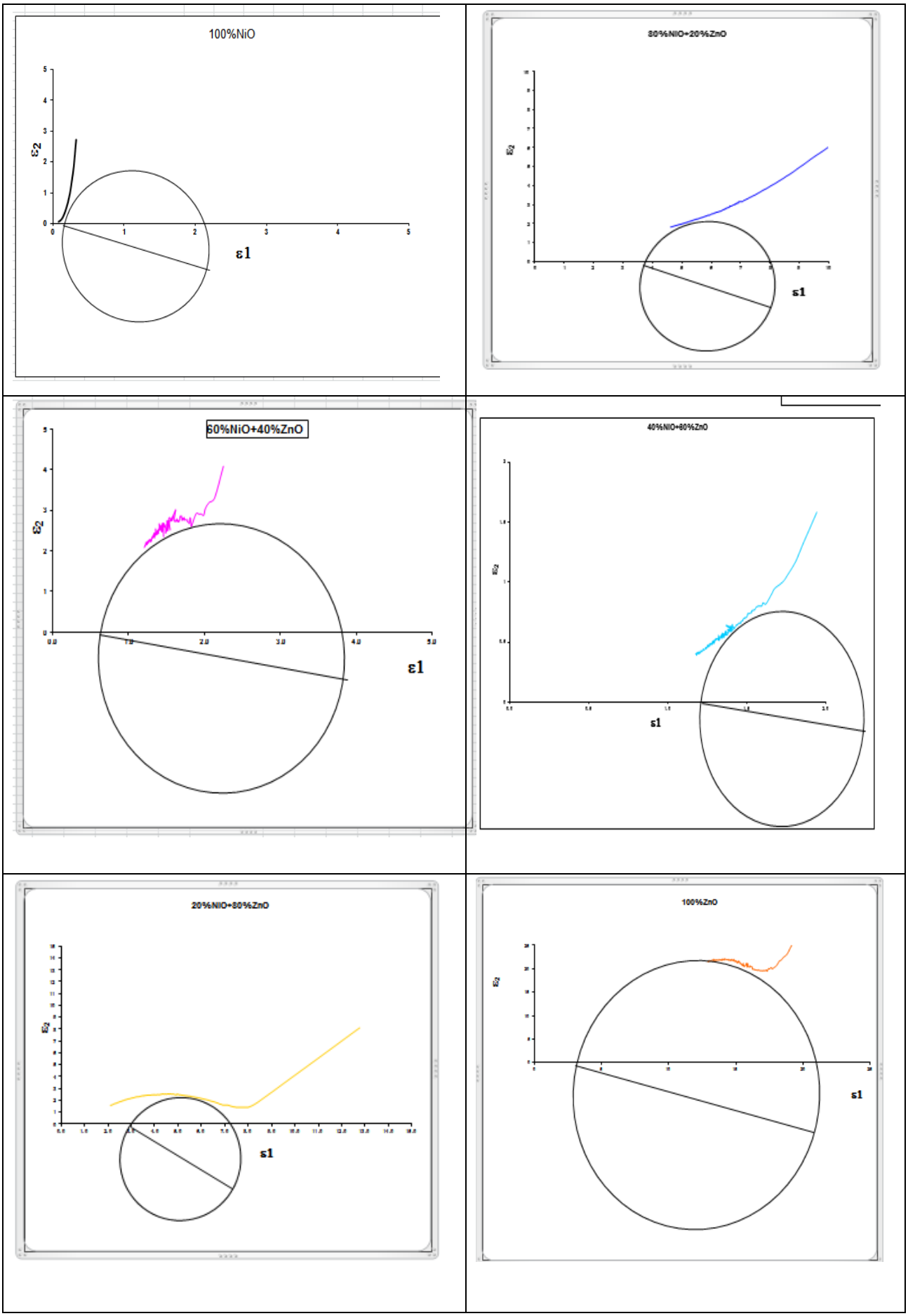

Figure 5: The plot of ε_1 versus ε_2 of (NiO/ZnO) with various ratios

Cole – Cole diagram of (NiO/ZnO) with various ratios

The most important proof of the existence of more than relaxation time of (NiO/ZnO) with different zinc oxide ratio can be obtained by drawing the dielectric constant $\varepsilon_1$versus dielectric loss ε_2 (Cole – Cole diagram) as shown in figure 5. The relations produced arc of circle where the center located below the x- axis. By measuring the angle formed between the diameter of the circle and x-axis, the polarizability (α) was determined and put in table 2. The values of (α) exhibit to change non systematically with zinc oxide ratio i.e., decreasing and increasing. The increase of (α) happen a result of reducing the intermolecular forces which take place when potential barrier was formed, while the reduction of (α) is due to the increment of intermolecular forces [19].

Conclusions

The results declare that a.c conductivity as well as ε_1 and ε_2 together were frequency dependent. The exponent s value was found very low for nickel oxide sample and close to unity for composites sample with high zinc oxide ratio. The estimated s values were found to increase but in non-regular manner with increasing of zinc oxide ratio. The conduction mechanism was proposed to be hopping between two sites within the CBH model. Interfacial and orientational polarization were responsible about frequency dependence of the dielectric constant ε_1. The barrier height and density were found to reduce while the density of states at Fermi level were was found to increase by increasing of zinc oxide ratio.

Recommendations

-Preparation of the compound using other techniques such as chemical spraying pyrolysis or RF-sputtering.

-Manufacturing a hybrid junction used in gas sensors or solar cells.

References

[1] R. Kanno, in Encyclopedia of Electrochemical Power Sources, 2009

[2] Qian L, Liu Z, Mo Y, Yuan H and Xiao D 2013 Mater. Lett. 100, 124–126.

[3] Wang Z L ACS Nano 2008 2 1987–92

[4] M.V. Kumar, T.G. Raja, N. Selvakumar, K. Jeyasubramanaian, this copy is for personal use only-distribution prohibited, Journal of References 95 Achievements in Materials and Manufacturing Engineering, 79 (2016) 13-18.

[5] Pollack M and Geballe T H 1961 Phys. Rev. 122 1742

[6] Ramana C V, Hussain O M, Naidu S S and Julien C 1999 Mater. Sci. Eng. B 60 173

[7] S.R. Elliott, Philos. Mag. 36, 1291 (1977).

[8] M. Kastener, H. Fritzsche, Philos. Mag. B 37, 199 (1978).

[9] M. Kastener, in: Proc. 7th Int. Conf. of Amorphous and Liquid Semiconductors, Ed. W.E. Spear, Edinburgh University 1977, p. 504.

[10] A.E. Streen, H. Eyring, J. Chem. Phys. 5, 113 (1937).

[11] J.C. Giuntini, J.V. Zanchetta, D. Jullien, R. Enolie, P. Houenou, J. Non-Cryst. Solids 45, 57 (1981).

[12] S.C. Agarwal, S. Guha, K.L. Narasimhan, J. Non- -Cryst. Solids 18, 429 (1975).

[13] M. Pollak, G.E. Pike, Phys. Rev. Lett. 25, 1449 (1972).

[14] S. Asokan, M.V.M. Prassad, G. Parathasarathy, E.S.R. Gopal, Phys. Rev. Lett. 62, 808 (1989).

[15] M. Barsoum, Fundamentals of Ceramics, Mc Graw--Hill, New York 1977, p. 543.

[16] N.F. Mott, E.A. Davis, R.A. Streel, Philos. Mag. 32, 961 (1975).

[17] M. Pollak, G.E. Pike, Phys. Rev. Lett. 28, 1494 (1972).

[18] S.R. Elliott, Solid State Commun. 27, 749 (1978).

[19] Ahmad A. Hasan, Iraqi Journal of Science, 2021, Vol. 62, No. 3, pp: 861-870 DOI: 10.24996/ijs.2021.62.3.17